Available online at www.sciencedirect.com
SCIENCE DIRECT
Thermochimica Acta 447 (2006) 184–189
thermochimica acta
www.elsevier.com/locate/tca

Synthesis and magnetic properties of $ZnFe_2O_4$ obtained by mechanochemically assisted low-temperature annealing of mixtures of Zn and Fe oxalates

V. Berbenni [a,*], C. Milanese [a], G. Bruni [a], A. Marini [a], I. Pallecchi [b]

[a] *CSGI, Dip. di Chimica-Fisica, Viale Taramelli, 16-27100 Pavia, Italy*
[b] *Dip. di Fisica, Via Dodecaneso, 33-16146 Genova, Italy*

Received 19 April 2006; received in revised form 5 June 2006; accepted 9 June 2006
Available online 16 June 2006

Abstract

The mechanism of formation of zinc ferrite ($ZnFe_2O_4$) from $ZnC_2O_4{\cdot}1.8H_2O$–$2Fe^{II}C_2O_4{\cdot}2H_2O$ and $ZnC_2O_4{\cdot}1.8H_2O$–$Fe_2^{III}(C_2O_4)_3{\cdot}6H_2O$ mixtures is investigated. By combination of TG and XRPD measurements it has been shown that microcrystalline $ZnFe_2O_4$ forms from physical mixtures after prolonged annealing at 1000 °C while nanocrystalline $ZnFe_2O_4$ powders are produced by mild annealing (1 h at 500 °C in air) of mechanically activated mixtures. The magnetic properties of $ZnFe_2O_4$ powders obtained from physical and from milled mixtures are compared.

Keywords: Zinc ferrite; Mechanical activation; Magnetic properties

1. Introduction

Ferrites are technologically important ceramic materials that have been studied and utilized for many years. Recently, the nanotechnology has spurred renewed interest in these materials. $ZnFe_2O_4$ crystallizes with a spinel lattice with Zn^{2+} in tetrahedral interstices and Fe^{3+} in the octahedral ones (direct spinel structure). Actually in nanosized ferrites it was observed that the distribution of cations in octahedral and tetrahedral sites changes as the crystallite size decreases [1] and that this fact leads to the unusual phenomenon of superparamagnetism on heating. Several synthetic routes to prepare nanosized $ZnFe_2O_4$ have been proposed. Besides the classical methods of coprecipitation [2], hydrothermal synthesis [3] and sol–gel [4], suitably modified methods have been proposed such as a synthetic route that, starting from metallic chloride solutions and using aqueous ammonia at pH 9 (180 °C), leads to 4 nm—$ZnFe_2O_4$ powders with magnetic susceptibility about two orders of magnitude higher than that of typical paramagnetic substances [5]. Furthermore, a modified coprecipitation synthesis process has been realized by heating under nitrogen a solution of Fe(II) sulphate and Zn(II) acetate with urea [6]. Again a wet synthesis starting from a solution of zinc chloride and iron(II) chloride [7] and a low temperature synthesis by using hydrazine monohydrate [8] have been performed. Finally direct mechanochemical synthesis has been realized starting from the constituent oxides ($ZnO + Fe_2O_3$) [9].

In the present work, we report a synthesis of nanometric $ZnFe_2O_4$ from a combination of mechanical activation of solid mixtures of metal oxalates [$ZnC_2O_4{\cdot}1.8H_2O + 2FeC_2O_4{\cdot}2H_2O$ or $ZnC_2O_4{\cdot}1.8H_2O + Fe_2(C_2O_4)_3{\cdot}6H_2O$] followed by mild annealing (1 h at 500 °C) under air flow. A study of the reaction mechanism has been performed by TG/DSC. Moreover, the dependence of the magnetic properties on the mechanical treatment is reported.

2. Experimental

2.1. Starting chemicals and samples preparation

The starting chemicals have been purchased by Aldrich Chimica (Italy): $ZnC_2O_4{\cdot}2H_2O$ (purity 99.9%), $FeC_2O_4{\cdot}2H_2O$ (purity 99.9%) and $Fe_2(C_2O_4)_3{\cdot}6H_2O$ (purity 99.9%). The

* Corresponding author. Fax: +39 0382 987575.
E-mail address: berbenni@matsci.unipv.it (V. Berbenni).

0040-6031/$ – see front matter © 2006 Elsevier B.V. All rights reserved.
doi:10.1016/j.tca.2006.06.006

hydration extent of the starting chemicals has been assessed by TG measurements: the number of water molecules of the two iron oxalates has been confirmed to coincide with the nominal one while that of the Zn compound resulted slightly less (1.81 versus 2). Physical mixtures (PM) of molar ratio Zn:Fe 1:2 have been prepared by weighing the appropriate amounts of the two components and by stirring them in acetone suspension for 3 h. Then the solvent has been evaporated in oven at 60 °C overnight. The mechanically activated mixtures (MM) have been prepared by dry milling lots of 2 g of the PM. The powders have been put into agate jars (12.5 mL) of a planetary mill (Pulverisette 7 by Fritsch, Germany) with three agate balls (12 mm diameter; ball/sample mass ratio 3:1). The mill has been operated at 500 rpm rotation speed for 50 h (1 h milling, 0.5 h pause). No addition of silica has been recorded by XRPD after the milling.

2.2. Experimental techniques

- TGA measurements have been performed by a 2950 thermogravimetric analyser (TA Instruments Inc., USA) connected to a TA 5000 computer (also by TA Instruments Inc., USA). Both PM and MM samples (about 50 mg) have been placed in a Pt–Rh pan and heated at 5 K/min (under air flow of 100 mL/min) from 25 °C up to 500 °C.
- Simultaneous DSC/TGA measurements have been performed with a STA 625 by Polymer Laboratories (UK) connected to a data station with proprietary software. Samples (≈10 mg) of MM have been placed in an aluminium pan and heated (under air flow of 120 mL/min) at 5 K/min from 25 °C up to 500 °C. The enthalpy values have been determined from the area of the DSC peaks recorded after calibration has been performed using sapphire (for heat capacity calibration) and indium–zinc (both for enthalpy and temperature calibration).
- X-ray powder diffraction patterns have been recorded in step scan mode (step 0.015°, 1 s/step, 40 kV, 30 mA) by a X-ray powder diffractometer (Bruker D5005) equipped with a Position Sensitive Detector (PSD, Braun). XRPD patterns have been recorded on the following samples: (i) samples of PM and MM recovered after the thermoanalytical scans in order to identify the compounds formed during thermal treatment; (ii) samples of both PM and MM heated (5 K/min under air flow) up to 500 °C and annealed for 1 h. The crystal size of $ZnFe_2O_4$ powders prepared from MM under air flow has been calculated by the Scherrer equation. The instrumental line broadening has been determined from the patterns of a $ZnFe_2O_4$ sample prepared from a physical mixture $ZnO–Fe_2O_3$ annealed 36 h at 1000 °C.
- Samples of both physical and milled mixtures have been examined by scanning electron microscopy (SEM, Model Stereoscan 200 by Cambridge, UK). Samples of $ZnFe_2O_4$ prepared by annealing MM have also been observed with SEM electron microscope. Before analysis all the samples have been sputtered under vacuum with gold metal.
- Specific surface area of both PM and MM has been determined by the BET method (N_2 adsorption, Sorptomatic 1990, Thermo Electron Corporation).
- Magnetic properties have been measured in a Quantum Design SQUID magnetometer. The magnetic moment as a function of temperature was measured in a magnetic field of 100 Oe. Hysteresis loop at different temperatures were measured in magnetic field up to 5 T.

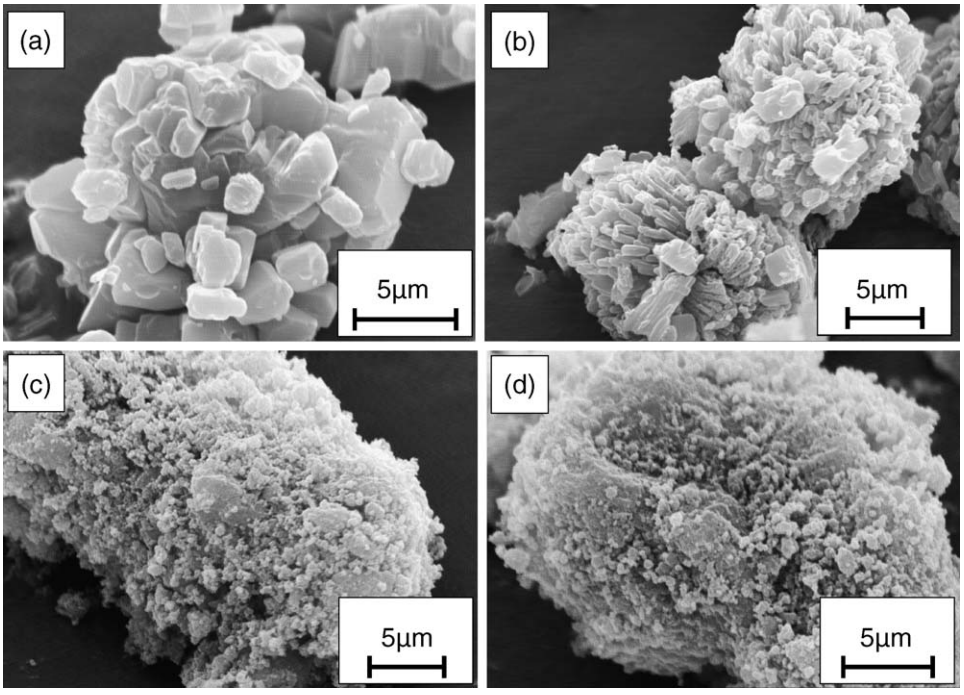

Fig. 1. SEM micrographs of (a) $ZnC_2O_4·1.8H_2O–2FeC_2O_4·2H_2O$ physical mixture; (b) $ZnC_2O_4·1.8H_2O–Fe_2(C_2O_4)_3·6H_2O$ physical mixture; (c) $ZnC_2O_4·1.8H_2O–2FeC_2O_4·2H_2O$ milled mixture; (d) $ZnC_2O_4·1.8H_2O–Fe_2(C_2O_4)_3·6H_2O$ milled mixture.

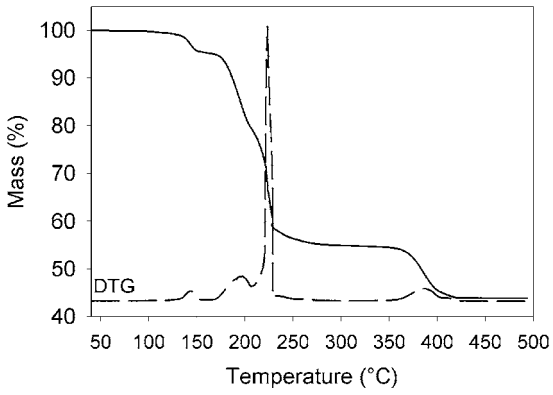

Fig. 2. TG (solid line) and DTG (dashed line) curves of $ZnC_2O_4{\cdot}1.8H_2O$–$2FeC_2O_4{\cdot}2H_2O$ physical mixture heated at 5 K/min up to 500 °C under air flow.

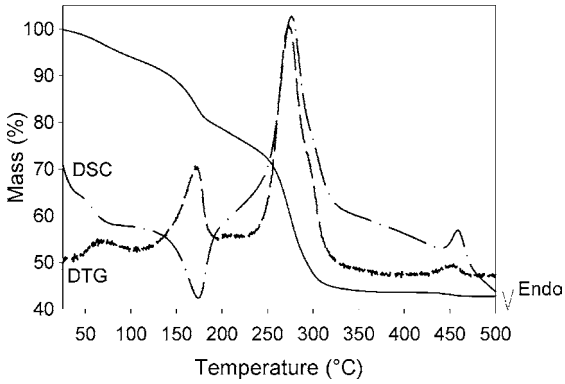

Fig. 3. TG (solid line), DTG (dashed line) and DSC (dashed-dotted line) curves of $ZnC_2O_4{\cdot}1.8H_2O$–$2FeC_2O_4{\cdot}2H_2O$ milled mixture heated at 5 K/min up to 500 °C under air flow.

3. Results and discussion

Fig. 1 reports the micrographs of samples of both physical (Fig. 1a and b) and milled (Fig. 1c and d) mixtures. The physical mixtures show differences in the crystal morphology depending on whether Fe(II) or Fe(III) oxalate is present. This should be the consequence of the fact that ferric oxalate was more agglomerated than the ferrous one. Another difference between the two types of mixtures is revealed by the fact that the specific surface area of the Fe(II) mixture (5.9 m^2/g) is three times larger that that of the Fe(III) mixture (1.9 m^2/g). The specific surface area of both mixtures increases by milling but the milling effect on the surface area is more evident on the Fe(III) mixture: the surface area of the Fe(II)-based mixture rises to 9.4 m^2/g (it increases by 1.5 times), whereas that of the Fe(III)-based mixture becomes 5.2 m^2/g (it increases almost three times). The higher effect of milling on the Fe(III) mixture is also evident when comparing the XRPD powder patterns of the milled mixtures. Some peaks, due to both oxalates, are indeed present in the Fe(II) mixture while complete amorphization has occurred in the Fe(III) mixture. A definite evidence of the fact that no oxalate decomposition has taken place during milling is obtained by a TG/DSC study of the processes occurring by heating the milled mixtures. Such study contributes to the understanding of the mechanism of the reaction.

3.1. Thermoanalytical measurements

3.1.1. $ZnC_2O_4{\cdot}1.8H_2O$–$2FeC_2O_4{\cdot}2H_2O$ mixtures

Fig. 2 shows a typical TG/DTG curve of a PM. The first step of mass loss (ending at ≈150 °C) is due to the dehydration of zinc oxalate. The second step ends at ≈300 °C and corresponds to a mass of 56.27 ± 0.44% (the standard deviation represents that of five independent measurements). During this step both Fe(II) oxalate dehydration and decomposition (with partial oxidation) occur. The mass value well agrees with that expected for the formation of a mixture ZnC_2O_4–(2/3)Fe_3O_4 (56.40%). The following step of mass loss (−12.19 ± 0.53%) is lower than that expected (−13.24%) for the decomposition of ZnC_2O_4 and this is due to the oxidation of Fe_3O_4 to Fe_2O_3 that takes place during the decomposition of ZnC_2O_4. Indeed the mean final mass value of 44.08 ± 0.44% well agrees with that expected for the formation of a mixture of ZnO and Fe_2O_3 (44.18%). The XRPD evidence confirms this point in that the reflexions present in the XRPD patterns of the residuals recovered from the TG runs are those characteristics of ZnO and Fe_2O_3 (no $ZnFe_2O_4$ has formed).

Fig. 3 shows a typical TG/DTG/DSC curve of a MM. It can be noted that the three mass loss steps are much less evident than in the case of the physical mixture. As concerns the first one, ending at ≈210 °C, the final mass of 77.75 ± 0.58% is obtained. Such a value is lower than that expected for the complete dehydration of the oxalates. The following mass loss steps quantitatively correspond to the decomposition of the anhydrous oxalates to a mixture ZnO–Fe_2O_3. The final mass value is 42.86% that is lower than the value expected. The XRPD patterns of the residuals recovered after the TG runs actually show the reflexions of $ZnFe_2O_4$ only. Therefore, the final mass lower than expected allows to state that absorption of volatile impurities occurs during milling. The mass value expected for the release of these impurities during heating and for the mixture dehydration is 78.43%, that fairly agrees with the mean experimental mass value reached at ≈210 °C (77.75 ± 0.58%).

As concerns the DSC curve, after the first endothermic peak due to the dehydration of the mixture, two exothermic peaks are showing up. The first one has an enthalpy (mean of five independent measurements) of −437.5 ± 48.0 kJ. The mean mass loss under this peak is the sum of the mass loss due to reaction:

$$2FeC_2O_{4(s)} + (3/2)O_{2(g)} \rightarrow Fe_2O_{3(s)} + 4CO_{2(g)} \quad (1)$$

and to the decomposition of a fraction of Zn oxalate (83.36 ± 6.34 mol%) according to the following equation:

$$0.8336ZnC_2O_{4(s)} \rightarrow 0.8336ZnO_{(s)} + 0.8336CO_{(g)} + 0.8336CO_{2(g)} \quad (2)$$

From the literature [10] the enthalpies of reactions (1) and (2) are, respectively, −278.15 kJ/mol FeC_2O_4 and +136.73 kJ/mol ZnC_2O_4. Therefore, the value expected for the enthalpy of the first exothermic peak is: (−278.15 kJ/mol FeC_2O_4) × 2 mol FeC_2O_4 + (+136.73 kJ/mol ZnC_2O_4) × 0.8336 mol ZnC_2O_4 =

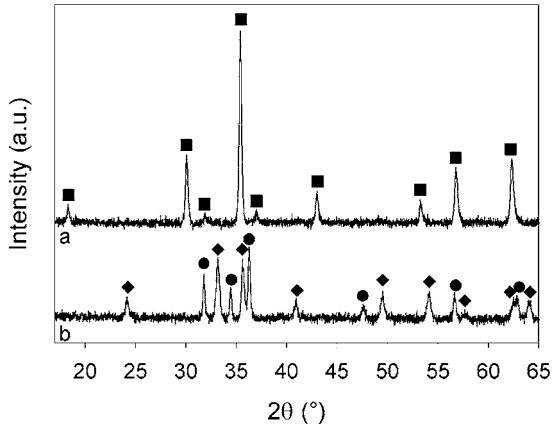

Fig. 4. XRPD patterns of $ZnC_2O_4{\cdot}1.8H_2O$–$2FeC_2O_4{\cdot}2H_2O$ mixtures heated at 5 K/min up to 500 °C under air flow: (a) milled mixture and (b) physical mixture. $ZnFe_2O_4$ (squares); ZnO (circles); Fe_2O_3 (lozenges).

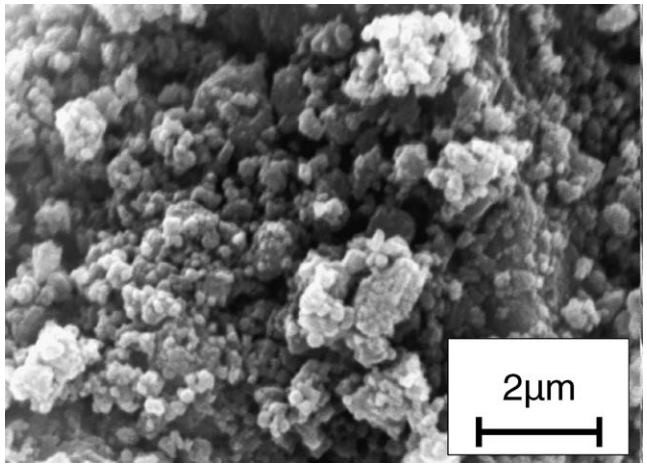

Fig. 5. SEM micrographs of $ZnC_2O_4{\cdot}1.8H_2O$–$2FeC_2O_4{\cdot}2H_2O$ milled mixture annealed 1 h at 500 °C in air.

−442.3 kJ that fairly agrees with the experimental value (−437.5 kJ).

As concerns the second exothermic peak the mean experimental enthalpy is -37.7 ± 2.5 kJ and the reaction under the peak is:

$$0.1664ZnC_2O_{4(s)} \rightarrow 0.1664ZnO_{(s)} + 0.1664CO_{(g)} + 0.1664CO_{2(g)} \quad (2')$$

So that the value expected for this peak is +22.8 kJ versus −37.7 kJ.

This means that an excess exothermic enthalpy of −60.5 kJ is present under the second exothermic peak that is related to the formation of $ZnFe_2O_4$.

The synthesis of $ZnFe_2O_4$ has been attempted by annealing (1 h) samples of MM at 500 °C: the mass loss at 500 °C (−57.59%) is in fair agreement with that obtained in TG analysis and the relevant XRPD patterns (Fig. 4a) of all the samples only show the reflexions of zinc ferrite though rather broad ones. By applying the equation of Scherrer to the XRPD line profile, the mean crystal size of 13.2 ± 1.6 nm has been calculated. The lattice constant of $ZnFe_2O_4$ obtained at 500 °C is 8.4355 ± 0.0056 Å, that is in fair agreement with that reported on the JCPDS file no. 022-1012 (8.4297 Å). The patterns of a sample of physical mixture subjected to the same thermal treatment (1 h at 500 °C) are shown in Fig. 4b: it can be seen that only the reflexions of both ZnO and Fe_2O_3 are present. An annealing at 1000 °C is needed to complete the $ZnFe_2O_4$ formation when starting from a physical mixture. The nanometric size of the MM sample calculated from XRD line broadening is confirmed by observing the SEM micrograph shown in Fig. 5.

3.1.2. $ZnC_2O_4{\cdot}1.8H_2O$–$Fe_2(C_2O_4)_3{\cdot}6H_2O$ mixtures

Fig. 6 shows a typical TG/DTG curve of a sample of PM: the first stage is a double one and the mean mass value at the first relative DTG minimum (≈200 °C) is 66.88 ± 1.51%.

As a matter of fact it is known from the literature [11,12] that the reduction of iron(III) oxalate to iron(II) oxalate occurs during the course of dehydration according to the following reaction:

$$Fe_2(C_2O_4)_3{\cdot}6H_2O_{(s)} \rightarrow 2FeC_2O_{4(s)} + 2CO_{2(g)} + 6H_2O_{(g)} \quad (3)$$

The mass value of 65.87% is to be expected if reaction (3) and zinc oxalate dehydration occur. The experimental mass value higher than expected can be justified if only a partial reduction of Fe(III) to Fe(II) would occur and, in this sense, the moles of iron(III) oxalate not reduced before ≈200 °C are 0.08.

The following stages show a total mean mass loss of -12.96 ± 0.55%. The separation between the two stages is rather poor. However, the XRPD patterns of the residuals show that a mixture ZnO–Fe_2O_3 has actually formed.

Fig. 7 shows a typical TG/DTG/DSC curve of a sample of MM. Also in the case of this milled mixture the mass loss steps are much less evident that in the physical mixture. No mass value corresponding to that expected if reaction (3) would occur can be individuated. Moreover the mass loss is over at a lower temperature than with the PM. The XRPD patterns of the residuals show only the peaks of $ZnFe_2O_4$.

As concerns the DSC traces, two exothermic peaks are present. The first one has an enthalpy (mean of six inde-

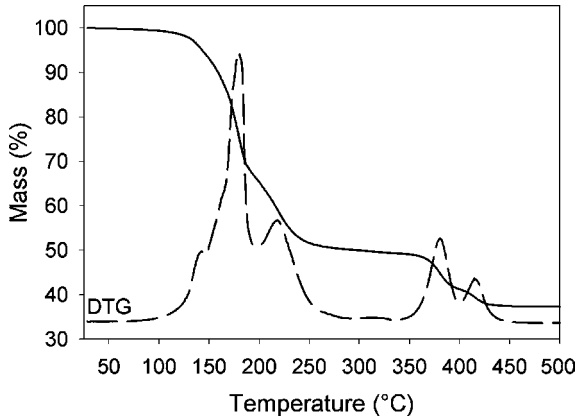

Fig. 6. TG (solid line) and DTG (dashed line) curves of $ZnC_2O_4{\cdot}1.8H_2O$–$Fe_2(C_2O_4)_3{\cdot}6H_2O$ physical mixture heated at 5 K/min up to 500 °C under air flow.

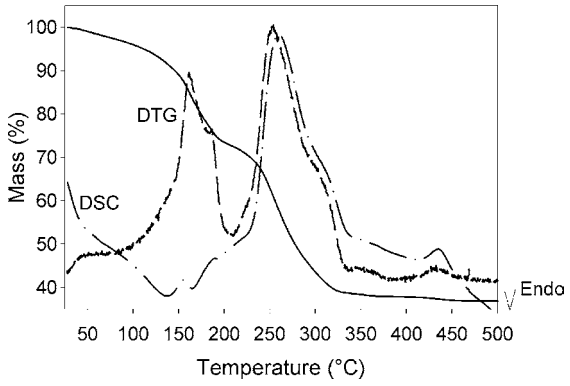

Fig. 7. TG (solid line), DTG (dashed line) and DSC (dashed-dotted line) curves of $ZnC_2O_4{\cdot}1.8H_2O$–$Fe_2(C_2O_4)_3{\cdot}6H_2O$ milled mixture heated at 5 K/min up to 500 °C under air flow.

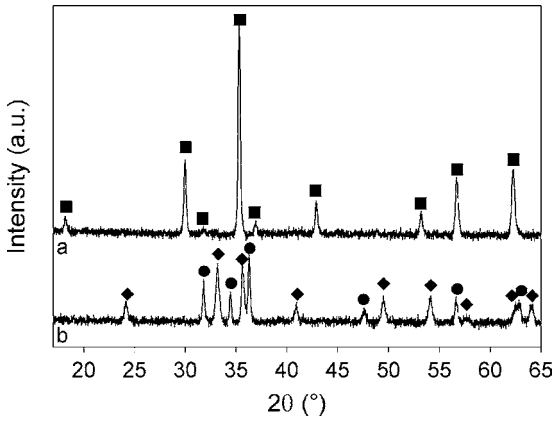

Fig. 8. XRPD patterns of $ZnC_2O_4{\cdot}1.8H_2O$–$Fe_2(C_2O_4)_3{\cdot}6H_2O$ mixtures heated at 5 K/min up to 500 °C under air flow: (a) milled mixture and (b) physical mixture. $ZnFe_2O_4$ (squares); ZnO (circles); Fe_2O_3 (lozenges).

pendent measurements) of -486.1 ± 44.2 kJ. The mass loss under the peak is a little lower than with the Fe(II)-based mixture. By hypothesizing that the reduction of Fe(III) oxalate to Fe(II) oxalate takes place, the enthalpy balance of the first exothermic peak can be set as follows: (−278.15 kJ/mol FeC_2O_4) × 2 mol FeC_2O_4 + (+136.73 kJ/mol ZnC_2O_4) × 0.7989 mol ZnC_2O_4 + $Y = -486.1$ kJ, with $Y = -39.0$ kJ.

The fact that in the case of the present reacting system, an excess of exothermic enthalpy is present also under the first peak means that some other process (very likely the Fe(III) oxalate reduction) is going on.

As concerns the second exothermic peak the mean experimental enthalpy is -39.0 ± 5.8 kJ and the reaction under the peak is:

$$0.2011ZnC_2O_{4(s)} \rightarrow 0.2011ZnO_{(s)} + 0.2011CO_{(g)} + 0.2011CO_{2(g)} \quad (2'')$$

So that the enthalpic balance under this peak is: -39.0 kJ = (0.2011 mol ZnC_2O_4) × (136.73 kJ/mol ZnC_2O_4) + Z, with $Z = -66.5$ kJ.

It can be noted that the excess of exothermic enthalpy under the second peak is nearly the same as that obtained (−60.5 kJ) with the Fe(II)-based mixture. Therefore, it is confirmed that an excess of exothermic enthalpy (−60.5 kJ) is related to the formation of $ZnFe_2O_4$.

$ZnFe_2O_4$ has been obtained from samples of milled mixture annealed in a furnace for 1 h at 500 °C (air). The relevant XRPD patterns of the sample only show the reflexions of zinc ferrite though rather broad ones (Fig. 8a). By applying the equation of Scherrer to the XRPD line profile, the mean crystal size of 14.2 ± 1.1 nm is obtained. The lattice constant of $ZnFe_2O_4$ obtained at 500 °C has been determined. The value of 8.4297 ± 0.002 Å is in fair agreement with that of $ZnFe_2O_4$ obtained starting from Fe(II) oxalate. The patterns of a sample of physical mixture subjected to the same thermal treatment (1 h at 500 °C) are shown in Fig. 8b: it can be seen that only the reflexions of both ZnO and Fe_2O_3 are present. An annealing at 1000 °C is needed to complete the $ZnFe_2O_4$ formation when starting from a physical mixture. The nanometric size of the MM sample calculated from XRD line broadening is confirmed by observing the SEM micrograph shown in Fig. 9.

4. Magnetic properties

The uppermost panel of Fig. 10 shows the magnetization as a function of temperature for powders of $ZnFe_2O_4$ obtained from:

(a) Mixture $ZnC_2O_4{\cdot}1.8H_2O$–$2FeC_2O_4{\cdot}2H_2O$ milled and annealed 1 h at 500 °C (sample 1).
(b) Mixture $ZnC_2O_4{\cdot}1.8H_2O$–$Fe_2(C_2O_4)_3{\cdot}6H_2O$ milled and annealed 1 h at 500 °C (sample 2).
(c) Mixture ZnO–Fe_2O_3 annealed 36 h at 1000 °C (sample 3).

It can be seen that all samples are paramagnetic at high temperature and anti-ferromagnetic below a temperature (T_N). For sample 3, the transition is broader and the transition temperature T_N is larger (nearly 60 K) that for samples 1 and 2 (nearly 35 K). It is well known that the normal $ZnFe_2O_4$ spinel has $T_N \approx 10$ K and it is also known that the partial inversion of spinel structure results in an increased T_N [13]. Hence, our data seem to indicate that sample 3 has a mixed spinel structure, whereas in

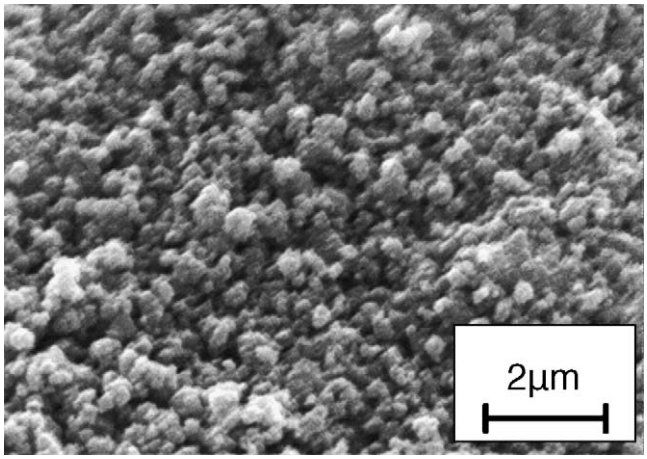

Fig. 9. SEM micrographs of $ZnC_2O_4{\cdot}1.8H_2O$–$Fe_2(C_2O_4)_3{\cdot}6H_2O$ milled mixture annealed 1 h at 500 °C in air.

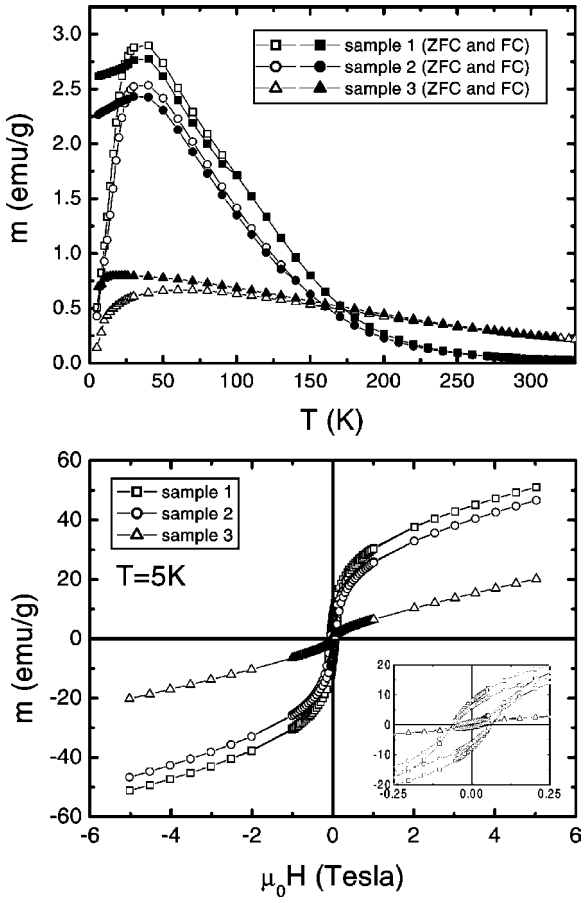

Fig. 10. Upper panel: magnetization as a function of temperature in an applied field of 100 Oe for sample 1 (squares), sample 2 (circles) and sample 3 (triangles). The open symbols are used for the zero field cooled curves, while the filled symbols are used for the field cooled curves. Lower panel: hysteresis loops of sample 1 (squares), sample 2 (circles) and sample 3 (triangles) measured at temperature 5 K. In the inset, a zoom of the low field region is presented, showing the enhanced coercive field of samples 1 and 2.

samples 1 and 2 the presence of the inverted spinel structure is less important.

The magnetization peak at the transition temperature for the three samples (at 100 Oe) is 2.9 emu/g (1), 2.5 emu/g (2) and 0.66 emu/g (3). These values are consistent with those reported for a nanocrystalline $ZnFe_2O_4$ powder [6].

Magnetic hysteresis loops have also been measured at different temperatures (5, 35, 100, 200 and 300 K) in magnetic fields up to 5 T. The lower panel of Fig. 10 shows the measurements at 5 K in the three samples. It can be seen that saturation is not yet attained even at 5 T, due to the presence of a linear and reversible contribution, which becomes increasingly preponderant with increasing temperature. Such behaviour indicates the presence of a paramagnetic phase, as it has already pointed out by other authors [6]. In the inset, a zoom of the low field region is shown, where it can be seen that at 5 K the coercive field is as large as 630 Oe for samples 1 and 2 and 320 Oe in the case of sample 3. The coercive field at 35 K, though small, has a finite value only in the case of samples (1 and 2) prepared starting from the milled mixtures. At higher temperatures, the coercive fields of all the samples are vanishingly small. Lopez et al. [14] synthesized nanocrystalline $ZnFe_2O_4$ powder with a remnant magnetization of 0.066 emu/g and a coercive field of 13 Oe; in comparison, the values of coercive fields found in our samples 1 and 2 are quite high. It seems that the synthetic procedure (milling + low temperature annealing) yields significant enhancement of the "pinning" of the magnetic domains, as a direct consequence of the sample microstructure.

5. Conclusions

- In order to synthesize $ZnFe_2O_4$, the solid state reactions in the systems $ZnC_2O_4{\cdot}2H_2O$–$2FeC_2O_4{\cdot}2H_2O$ and $ZnC_2O_4{\cdot}2H_2O$–$Fe_2(C_2O_4)_3{\cdot}6H_2O$ have been studied. Independently on the iron precursor selection (Fe^{2+} or Fe^{3+}). It has been shown that the mechanical activation of the starting systems results in the formation of $ZnFe_2O_4$ within 500 °C while only a mixture ZnO–Fe_2O_3 is produced when starting from the unmilled mixtures. The enthalpy of $ZnFe_2O_4$ formation starting from the constituent oxides has been estimated.
- One hour-annealing of the activated mixtures at 500 °C in air yields nanocrystalline $ZnFe_2O_4$ while prolonged annealing at 1000 °C is needed to obtain microcrystalline $ZnFe_2O_4$ when starting from the corresponding non-activated systems.
- The proposed synthetic procedure (milling + low temperature annealing) yields significant enhancement of the "pinning" of the magnetic domains, as a direct consequence of the sample microstructure.

References

[1] T. Kamiyama, K. Haneda, T. Sato, S. Ikeda, H. Asano, Solid State Commun. 81 (1992) 563.
[2] T. Sato, K. Haneda, M. Seki, T. Iijima, Appl. Phys. A 50 (1990) 13.
[3] S.-H. Yu, T. Fujino, M. Yoshimura, J. Magn. Magn. Mater. 256 (2003) 420.
[4] S. Li, L. Wang, J.B. Wang, Q.G. Zhou, X.Z. Zhou, H.P. Kunkel, G. Williams, J. Magn. Magn. Mater. (2004) 332.
[5] C. Upadhyay, H.C. Verma, C. Rath, K.K. Sahu, S. Arnaud, R.D. Dasi, N.C. Mishra, J. Alloy Compd. 326 (2001) 94.
[6] K. Animesh, C. Upadhyay, H.C. Verma, Phys. Lett. A 311 (2003) 410.
[7] M. Ueda, S. Shimada, M. Inagaki, J. Mater. Chem. 3 (12) (1993) 1199.
[8] M. Ueda, S. Shimada, M. Inagaki, J. Eur. Ceram. Soc. 15 (1995) 265.
[9] S. Bid, S.K. Pradhan, Mater. Chem. Phys. 82 (2003) 372.
[10] R. Majumdar, P. Sarkar, U. Ray, M.R. Mukhopadhyay, Thermochim. Acta 335 (1999) 43.
[11] A.K. Galwey, M.A. Mohamed, Thermochim. Acta 213 (1993) 279.
[12] M.A. Mohamed, A.K. Galwey, Thermochim. Acta 213 (1993) 265.
[13] G.F. Goya, H.R. Rechenberg, J. Magn. Magn. Mater. 196 (1999) 191.
[14] F.A. Lopez, A. Lopez-Delgado, J.L.M. de Vidales, E. Vila, J. Alloy Compd. 265 (1998) 291.